This article has been accepted for publication in a future issue of this journal, but has not been fully edited. Content may change prior to final publication. Citation information: DOI10.1109/TVT.2022.3232841, IEEE Transactions on Vehicular Technology

UAV-Aided Vehicular Short-Packet Communication and Edge Computing System under Time-Varying Channel

Shuai Shen, Kun Yang, *Senior Member, IEEE,* Kezhi Wang, *Senior Member, IEEE,* and Guopeng Zhang,

***Abstract*—In this paper, a novel UAV-aided vehicular edge computing (VEC) network is proposed, where the vehicle and on-board UAV provide multi-access edge computing (MEC) service for the roadside Internet of Things (IoT) devices. In this system, considering the time-varying channel, we derive the lower bound of signal-to-noise ratio (SNR) based on the first-order Gauss-Markov process. Then, with the short-packet transmission, we maximize the total amount of computation by jointly optimizing the communication scheduling, the trajectories of the vehicle and on-board UAV, and the computing resource, subject to the mobility, connection and computation constraints. The formulated optimization problem is a mix-integer non-convex problem. To efficiently solve it, we propose an alternative algorithm based on the Lagrangian dual decomposition and successive convex approximation technique. Extensive simulation results are provided to show the performance gain of the proposed algorithm.**

***Index Terms*—Multi-access edge computing, vehicular network, unmanned aerial vehicle, time-varying channel, short-packet communication.**

I. Introduction

A. Background and Motivation

THE explosive increase in the number of devices results in massive communication traffic and computation-intensive applications in the Internet of Things (IoT) network [1]. Multi-access edge computing (MEC) has been proposed to relieve the backhaul load for the network and reduce the round-trip latency for the resource-constrained devices [2]. Moreover, vehicles now are able to communicate with the roadside units and exploit their resource to enhance the conventional MEC networks [3]. The system where vehicles participate in MEC is called vehicular edge computing (VEC) system, which has been widely investigated recently.

Although the VEC system can mitigate the load of the edge access point, the shortage of spectrum and computing resource still exists. This is caused by the nature of vehicle. First, since the roads are fixed, the routes of the vehicle are limited. As a result, it is difficult to provide high-quality service for the IoT devices far from the road. Second, restricted by the size of vehicle, its computing and storage resources are limited. Fortunately, unmanned aerial vehicles (UAV), as the mobile and flexible equipment, can effectively overcome these shortages. They can fly close to the devices to provide high-quality service, and supplement the computing resource for the VEC system.

As a hot research direction, the UAV has been widely exploited in MEC systems [4]–[6]. However, the research on the UAV-aided VEC system is still in its infancy. In most existing literature, the UAVs only execute the computational tasks offloaded from the vehicles. There is no cooperation between the vehicles and UAVs. How to exploit the communication and computing resource of the vehicles and UAVs to process the data offloaded from the roadside IoT devices still needs efforts.

Due to the mobility of the vehicle and UAV, the latency and reliability of data transmission are of great importance. Untimely data uploading may lead to the expiration or even loss of the information, thus causing serious consequences. To meet the latency and reliability requirements, short-packet communication is applied in vehicle and UAV systems, which focuses on conveying sensing information, control command, and feedback information in short packets [7]. It can support high reliability with a packet error rate (PER) around 10^{-5} and very low latency less than 1 ms [8]. Due to the excellent advantages, plenty of literature has studied the application of short-packet communication in MEC systems. Moreover, it has been shown that the UAV-mounted base station (BS) is more feasible than the fixed terrestrial BS to realize short-packet communication by exploiting spatial diversity [7]. Therefore, short-packet communication is now a prevalent direction in UAV-assisted communication network.

Moreover, in most of the recent work, the channel state information (CSI) of the vehicle and UAV is assumed to be perfectly known, which is impractical for the vehicle and UAV communication systems. In practical applications, the mobility

This work was supported in part by the MOST Major Research and Development Project under Grant No. 2021YFB2900204, in part by the Natural Science Foundation of China under Grant No. 62132004, in part by the Sichuan Major R&D Project under Grant No. 22QYCX0168, in part by Quzhou Government under Grant No. 2021D003, and in part by Sichuan Major R&D Project under Grant No.: 2021YFG0363.

Shuai Shen is with the School of Information and Communication Engineering, University of Electronic Science and Technology of China, Chengdu 611731, China (e-mail: shuaishen@std.uestc.edu.cn).

Kun Yang is with School of Information and Communication Engineering, University of Electronic Science and Technology of China, Chengdu 611731, China, and also with the Yangtze Delta Region Institute, University of Electronic Science and Technology of China, Quzhou 324000, China (e-mail: kyang@ieee.org).

Kezhi Wang is with Department of Computer Science, Brunel University London, Uxbridge, Middlesex, UB8 3PH (email: kezhi.wang@brunel.ac.uk).

Guopeng Zhang is with the School of Computer Science and Technology, China University of Mining and Technology, Xuzhou 221116, China (email: gpzhang@cumt.edu.cn).

This article has been accepted for publication in a future issue of this journal, but has not been fully edited. Content may change prior to final publication. Citation information: DOI10.1109/TVT.2022.3232841, IEEE Transactions on Vehicular Technology

of the vehicle and UAV generates the dynamic environment and leads to time-varying channels [9] [10]. While the vehicle and the UAV move, the channels change rapidly. To achieve the accurate channel estimation, the CSI has to be updated quite often, which is challenging to realize [11]. In addition, CSI acquisition generally requires downlink pilot transmission followed by uplink feedback. As a result, the excessive use of downlink pilots entails a large communication overhead to feed back the estimated CSI from the devices to the vehicle and the UAV [12]. In summary, the frequent channel estimation is difficult and costly in the vehicle and UAV communication systems. Therefore, to study the UAV-aided vehicle communication system more practically, the time-varying channel needs to be considered.

B. Our Contribution

Different from the above work assuming perfect channel estimation and infinite packet length, this paper investigates the UAV-aided vehicular short-packet communication and edge computing system in time-varying channel, which imposes the following new challenges.

1) The vehicle-mounted UAV is released by the vehicle, and flies back eventually. They cooperate in processing the computational data offloaded from the roadside IoT devices. Therefore, the collaboration between the vehicle and the on-board UAV needs to be considered.
2) In the time-varying channel caused by the mobility of the vehicle and the UAV, the channels vary rapidly. The accurate CSI needs frequent channel detection, which is infeasible. Thus, the signal-to-noise (SNR) is difficult to obtain.
3) The non-convexity of the achievable rate in the short-packet communication is challenging to address. The time-varying channel further increases the difficulty.

We aim to address these challenges in this paper. Our goal is to maximize the total amount of computation by jointly optimizing the communication scheduling, the trajectories of the vehicle and the on-board UAV, and the computing resource, subject to the mobility, connection and computation constraints. To solve this mix-integer non-convex optimization problem, we propose an alternative algorithm to obtain a high-quality solution. The main contributions of this paper are summarized as follows.

1) We propose a novel UAV-aided VEC system architecture, in which the vehicle releases the on-board UAV to provide MEC service for the roadside IoT devices. The UAV can process the computational data offloaded from the devices that can not achieve high-quality service from the vehicle, thus improving the total amount of computation. Eventually, the UAV needs to return to the vehicle.
2) We consider the practical time-varying channel, in which the subsequent CSI can be estimated by that of the previous moment through the first-order Gauss-Markov process. Then, we derive the lower bound of SNR in time-varying Rician fading channel. To guarantee the amount of computation, we investigate the optimization problem based on the derived lower bound of SNR.

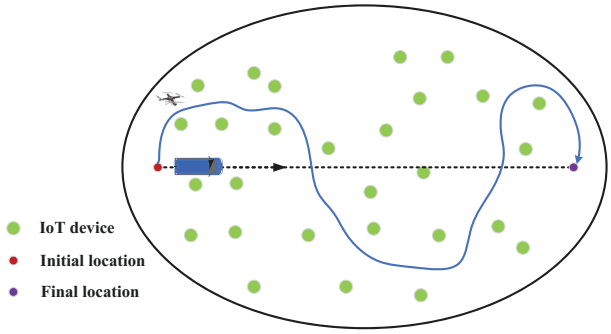

Fig. 1. UAV-aided VEC network.

3) We formulate the computation maximization problem based on short-packet communication. This is a mix-integer non-convex optimization problem, which is difficult to solve directly. To efficiently obtain the high-quality solution, we decompose the optimization problem into two subproblems: the communication scheduling, and the trajectory and computing resource optimization problems. The first subproblem is an integer programming problem. To solve it efficiently, we propose a low-complex algorithm based on the Lagrangian dual decomposition method. The second subproblem is also a non-convex problem due to the property of short-packet communication. We first transform it into a more tractable one, and then solve it through successive convex approximation (SCA) technique. Finally, by combining the solutions of these two subproblems, we propose an alternative algorithm.

The reminder of this paper is organized as follows. Section II introduces the related work. In Section III, the UAV-aided VEC system is proposed and the optimization problem is formulated. The proposed algorithms are presented in Section IV. Section V provides numerical results to verify the performance of the proposed algorithm, and analyze the features of the system. The conclusion is drawn in Section VI. The main notations used in this paper are summarized in Table I.

II. Related Work

To meet the rising demand for intelligent applications, such as autonomous driving, current vehicles are endowed with powerful computing capacity [13]. This prompts vehicles to be the computing service providers in VEC systems, similar to the edge servers in MEC systems. Although the mobility of vehicle improves the experience of the devices, it also results in the fast varying network topology, wireless channel state and computing workload. Focusing on the dynamic vehicular tasks offloading environment, Sun *et al.* proposed an adaptive learning based task offloading algorithm through the multi-armed bandit theory [13]. Moreover, for the dynamic vehicular environment, the reliable communication and computation is of great importance. To improve the cooperative vehicle-to-vehicle communication and computation reliability, Han *et al.* established an optimal partition model and proposed a coupling-oriented reliability calculation by dynamic program-

This article has been accepted for publication in a future issue of this journal, but has not been fully edited. Content may change prior to final publication. Citation information: DOI10.1109/TVT.2022.3232841, IEEE Transactions on Vehicular Technology

TABLE I
SUMMARY OF NOTATIONS

Parameter	Description
K	Number of IoT devices
T	Vehicle travel time duration
N	Number of time slots
δ	Time slot length
ρ_0	Channel power gain at the reference distance of 1m
B	Channel bandwidth
α	Temporal fading coefficient
β_j	Rician factor
ϵ	Decoding error probability
σ_h^2	Variance of channel estimation error
σ_z^2	Noise power at the receiver
$\mathbf{w}_i$	Location of the i-th IoT device
P_i	Transmit power of the i-th IoT device
C_i	Required CPU cycles for computing 1 bit data of the i-th IoT device
$\mathbf{q}_I$	Initial location of the vehicle
$\mathbf{q}_F$	Final location of the vehicle
$\mathbf{q}_j$	Horizontal coordinates of the vehicle ($j=0$) and the UAV ($j=1$)
H_j	Height of the vehicle or the UAV
f_j^{max}	Maximum CPU frequency of the vehicle or the UAV
V_j^{max}	Maximum speed of the vehicle or the UAV
$d_{ij}[n]$	Distance between the i-th IoT device and the vehicle or the UAV in the n-th time slot
$g_{ij}[n]$	Large-scale fading coefficient between the i-th IoT device and the vehicle or the UAV in the n-th time slot
$\zeta_{ij}[n]$	Small-scale fading coefficient between the i-th IoT device and the vehicle or the UAV in the n-th time slot
$a_{ij}[n]$	Communication scheduling variable for the i-th IoT device in the n-th time slot
$f_{ij}[n]$	CPU frequency allocated to the i-th IoT by the vehicle or the UAV in the n-th time slot

ming methods [14]. According to the cooperation between vehicles as well as between vehicles and roadside units, Xu *et al.* studied the joint communication, caching and computing resource allocation of the content sharing problem and proposed a caching strategy based on the popularity and social similarity [15]. Similarly, in collaborative VEC systems, Huang *et al.* investigated the contact based incentive mechanism to utilize the computing resource of parked vehicles to serve the offloading user [16]. However, aside from the efficiency, the cooperation also introduces the security and privacy issues into VEC systems. To address these problems, Cui *et al.* proposed a security and privacy-preserving cooperative downloading scheme based on the edge computing [17].

Since the roads are fixed and the computing resource of the vehicles is limited, they may not provide high-quality service for every device. Owing to the flexibility, the UAV becomes a solution to this issue. However, there are few researches on the UAV-aided VEC systems at present. In [18], Cheng *et al.* showed the advantages of employing UAV in the VEC system and proposed a novel aerial-ground integrated MEC architecture. To reduce the task execution time and system energy consumption, Zhao *et al.* proposed an SDN-enabled UAV-assisted vehicular computation offloading framework and designed a computation cost optimization algorithm [19]. Moreover, Zhao *et al.* also investigated the UAV-aided VEC system in industrial IoT networks, considering the execution time, the energy consumption and the computing resource rental price [20]. With regard to the resource allocation problem, Peng *et al.* studied a distributive multi-dimensional resource management scheme and proposed a multi-agent deep deterministic policy gradient based method to maximize the number of offloaded tasks from the vehicles while meeting their heterogeneous quality-of-service (QoS) requirements [21].

Due to the low latency and high reliability of short-packet communication, it has received much attention in MEC field [22]–[24]. In a multi-user MEC architecture where multiple servers have heterogeneous computing resources, Liu *et al.* proposed a short-packet communication based task offloading and resource allocation framework considering the statistics of extreme queue length events [22]. Through establishing the digital twin of the real MEC system, Dong *et al.* proposed a deep learning framework to reduce the energy consumption of short-packet communication and delay tolerant services [23]. By leveraging Lyapunov optimization, Zhou *et al.* proposed a learning-based task offloading approach for the MEC system with short-packet communication constraints [24]. Different from the conventional systems, the UAV-aided communication systems can provide mobile and flexible services. In this case, short-packet communication is more necessary and suitable. In [25], Wang *et al.* investigated the average packet error probability and effective throughput of the UAV short-packet communication system. She *et al.* established a framework for enabling the short-packet communication in the control and non-payload communication links of the UAV communication system [26]. Chen *et al.* investigated the resource allocation and the UAV deployment in the UAV-assisted short-packet communication service system [27]. To improve the transmission rate of backward link, Cai *et al.* also studied the resource allocation in a short-packet communication enabled two-way UAV relaying system [28].

III. SYSTEM MODEL AND PROBLEM FORMULATION

In this section, we first propose a time-varying UAV-aided VEC system architecture and introduce the system model. Then, the computation maximization problem is formulated.

A. UAV-Aided VEC System

As shown in Fig. 1, in the time-varying UAV-aided VEC network, the vehicle, carrying a MEC server and an on-board UAV, provides MEC service for the roadside IoT devices. When the computing resource of the vehicle is insufficient or the devices are far from the vehicle, the QoS will deteriorate. To address this issue, the vehicle releases the on-board UAV, which also carries a MEC server, to improve the service experience of the devices. Since the mobility of the vehicle and UAV results in the time-varying channel, the CSI of every moment can not be perfectly known. To acquire the accurate CSI, the vehicle needs to transmit pilot signals to the devices. Then, the devices transmit the received information back to the vehicle, which thus obtains the CSI. In this system, the vehicle transmits pilot signals to obtain the accurate CSI before releasing the UAV. Then, the subsequent CSI needs to be estimated through the first-order Gauss-Markov process. After the channel estimation, the trajectories of the vehicle

and the UAV, the communication scheduling and the resource allocation are jointly designed in the vehicle according to the estimated CSI. Then, the vehicle transmits the results to the on-board UAV and the IoT devices through dedicated control channels. The devices and the UAV execute the offloading and computing tasks according to the received results. To support the latency-critical tasks, such as emergency rescue, target tracking and perception, short-packet communication is adopted in this system. The IoT devices offload t he computational data in short packet size to guarantee the low-latency transmission.

B. System Model

In this paper, we focus on the single vehicle system[1], where a vehicle and its on-board UAV provide MEC service for K IoT devices within a given time duration of T, as shown in Fig 1. The set of the IoT devices is denoted as $\mathcal{K}$, and thus we have the cardinality $|\mathcal{K}| = K$. It is assumed that the vehicle obtains the accurate CSI of the network at the initial point through pilot transmission. Without loss of generality, the locations of the IoT devices are represented by the three-dimensional (3D) Cartesian coordinates $(\mathbf{w}_i^T, 0)$, $\forall i \in \mathcal{K}$, where $\mathbf{w}_i = [x_i, y_i]^T \in \mathbb{R}^{2\times 1}$ denotes the horizontal coordinate of the i-th IoT device. It is assumed that the initial and final locations of the vehicle are predetermined, denoted as $(\mathbf{q}_I^T, 0)$ and $(\mathbf{q}_F^T, 0)$, respectively, where $\mathbf{q}_I = [x_I, y_I]^T \in \mathbb{R}^{2\times 1}$ and $\mathbf{q}_F = [x_F, y_F]^T \in \mathbb{R}^{2\times 1}$ are the corresponding horizontal coordinates.

For ease of analysis, the time horizon T is discretized into N equal time slots, indexed by $\mathcal{N} = \{1, ..., N\}$. The slot length $\delta = \frac{T}{N}$ is chosen sufficiently small such that the locations of the vehicle and the UAV can be approximated as unchanged within each time slot. It is also assumed that the vehicle-mounted UAV is released at the initial location, flies at a fixed altitude H_1 above ground, and return to the vehicle at the final location. As such, the trajectories of the vehicle and the UAV can be approximated by the $(N+1)$-length 3D sequence $(\mathbf{q}_0^T[n], H_0)$ and $(\mathbf{q}_1^T[n], H_1)$, respectively, where $\mathbf{q}_0[n] = [x_0[n], y_0[n]]^T \in \mathbb{R}^{2\times 1}$ and $\mathbf{q}_1[n] = [x_1[n], y_1[n]]^T \in \mathbb{R}^{2\times 1}$ denote the corresponding horizontal coordinates, and H_0 represents the height of the vehicle. Moreover, the maximum speeds of the vehicle ($j = 0$) and UAV ($j = 1$) are denoted as V_j^{max}, $j \in \{0, 1\}$, in meter/second (m/s), and their maximum CPU frequencies are denoted as f_j^{max} in Hertz (Hz).

Generally, there are five main differences between the vehicle and the UAV:

1) The vehicle can only travel on the fixed route, but the UAV can fly anywhere.
2) The height of the vehicle is less than that of the UAV, i.e., $H_0 < H_1$.
3) To guarantee that the UAV can return to the vehicle at the final location, the vehicle can not move too fast. Therefore, its maximum speed is less than that of the UAV, i.e., $V_0^{max} < V_1^{max}$.
4) Restricted by the size of UAV, its maximum CPU frequency is less than that of the vehicle, i.e., $f_0^{max} > f_1^{max}$.
5) Due to the difference between the aerial and the ground environments, the LoS channel component of the vehicle-device link is less than that of the UAV-device links, i.e. $\beta_0 < \beta_1$.

For the purpose of exposition, we assume that the vehicle moves along a straight line from the initial location to the final location, as shown in Fig 1. Therefore, we have

$$\mathbf{q}_j[1] = \mathbf{q}_I, \mathbf{q}_j[N+1] = \mathbf{q}_F, \forall j \in \{0, 1\}, \tag{1}$$

$$y_0[n] = \frac{y_F - y_I}{x_F - x_I}(x_0[n] - x_I) + y_I, n \in \mathcal{N}. \tag{2}$$

Then, the maximum moving distances of the vehicle and the UAV within each time slot are given by $S_j = V_j^{max}\delta$, $j \in \{0, 1\}$. As a result, the speed constraints of the vehicle and the UAV can be expressed as

$$\|\mathbf{q}_j[n+1] - \mathbf{q}_j[n]\| \leq S_j, \forall j \in \{0, 1\}, n \in \mathcal{N}. \tag{3}$$

C. Time-varying Channel Model

Based on the above coordinates, the distances between the i-th IoT device and the vehicle ($j = 0$) as well as the UAV ($j = 1$) in the n-th time slot can be expressed as

$$d_{ij}[n] = \sqrt{\|\mathbf{q}_j[n] - \mathbf{w}_i\|^2 + H_j^2}. \tag{4}$$

Therefore, the large-scale fading coefficients of the vehicle-device and UAV-device links are given by

$$g_{ij}[n] = \sqrt{\rho_0 d_{ij}^{-2}[n]} = \sqrt{\frac{\rho_0}{\|\mathbf{q}_j[n] - \mathbf{w}_i\|^2 + H_j^2}}, \tag{5}$$

where ρ_0 denotes the channel power gain at the reference distance of $d_0 = 1$ m.

Besides the large-scale fading, we also consider the small-scale fading in the vehicle-device and UAV-device links, which are assumed to be time-varying channels. As mentioned above, based on the first-order Gauss-Markov process, the vehicle predicts the subsequent CSI by that of the previous moment. Therefore, the small-scale fading coefficients can be expressed as [29]

$$\begin{aligned}\zeta_{ij}[n] &= \sqrt{\alpha}\zeta_{ij}[n-1] + \sqrt{1-\alpha}\phi_{ij}[n] \\ &= \alpha^{\frac{n}{2}}\zeta_{ij}[0] + \sqrt{1-\alpha}\sum_{k=1}^{n}\alpha^{\frac{n-k}{2}}\phi_{ij}[k],\end{aligned} \tag{6}$$

where α characterizes the temporal fading coefficient with the range of $[0, 1]$, and $\phi_{ij}[n]$ follows the independent and identically distributed (i.i.d.) circularly symmetric complex Gaussian (CSCG) distribution with zero mean and σ_h^2 variance, i.e., $\phi_{ij}[n] \sim \mathcal{CN}(0, \sigma_h^2)$.

Due to the existence of the LoS path, the accurate small-scale fading at the first moment can be modeled by the Rician fading as

$$\zeta_{ij}[0] = \sqrt{\frac{1}{\beta_j + 1}}\widetilde{\xi}_{ij} + \sqrt{\frac{\beta_j}{\beta_j + 1}}\overline{\xi}_{ij}, \tag{7}$$

[1]Although this paper only focuses on the single-vehicle and single-UAV system, the considered model is practical and general. Therefore, the proposed algorithm can also be applied in the multi-vehicle and multi-UAV system through expanding the communication scheduling variables.

This article has been accepted for publication in a future issue of this journal, but has not been fully edited. Content may change prior to final publication. Citation information: DOI10.1109/TVT.2022.3232841, IEEE Transactions on Vehicular Technology

where $\widetilde{\xi}_{ij} \sim \mathcal{CN}(0,1)$ denotes the random scattered component which is i.i.d. CSCG random variables with zero mean and unit variance, $\bar{\xi}_{ij}$ represents the deterministic LoS channel component with $|\bar{\xi}_{ij}| = 1$, and β_j is the Rician factor.

Therefore, the channel coefficients of the vehicle-device and UAV-device links are given by

$$h_{ij}[n] = g_{ij}[n]\zeta_{ij}[n] = \overline{h}_{ij}[n] + \widetilde{h}_{ij}[n], \tag{8}$$

where

$$\overline{h}_{ij}[n] = \alpha^{\frac{n}{2}}\left(\frac{\beta_j}{\beta_j+1}\right)^{\frac{1}{2}} g_{ij}[n]\bar{\xi}_{ij}, \tag{9}$$

$$\widetilde{h}_{ij}[n] = \alpha^{\frac{n}{2}}\left(\frac{1}{\beta_j+1}\right)^{\frac{1}{2}} g_{ij}[n]\widetilde{\xi}_{ij} + (1-\alpha)^{\frac{1}{2}} g_{ij}[n]\sum_{k=1}^{n}\alpha^{\frac{n-k}{2}}\phi_{ij}[k]. \tag{10}$$

Since $\phi_{ij}(t) \sim \mathcal{CN}(0,\sigma_h^2)$ and $\widetilde{\xi}_{ij} \sim \mathcal{CN}(0,1)$, one can have $\widetilde{h}_{ij}[n] \sim \mathcal{CN}(0, (\frac{\alpha^n}{\beta_j+1} + \sigma_h^2(1-\alpha^n))g_{ij}^2[n])$, i.e., the variance of $\widetilde{h}_{ij}[n]$ is $\sigma^2_{\widetilde{h}_{ij}[n]} = (\frac{\alpha^n}{\beta_j+1} + \sigma_h^2(1-\alpha^n))g_{ij}^2[n]$.

It can be seen from equation (6) that the subsequent CSI is estimated according to the accurate CSI obtained before the vehicle releases the on-board UAV. In order to guarantee the amount of computation, we formulate the optimization problem based on the worst case of prediction. Assume that the i-th IoT device offloads computational data with a constant transmit power P_i when it is scheduled for communication. Then, we have the following lemma.

Lemma 1: The lower bound of signal-to-noise ratio (SNR) in time-varying Rician fading channel between the i-th IoT device and the vehicle as well as the UAV in the n-th time slot is expressed as

$$\Gamma_{ij}[n] = \frac{P_i\bar{h}_{ij}^2[n]}{P_i\sigma^2_{\widetilde{h}_{ij}[n]} + \sigma_z^2} = \frac{\gamma_{ij}[n]}{\sigma_z^2\|\mathbf{q}_j[n] - \mathbf{w}_i\|^2 + \eta_{ij}[n]}, \tag{11}$$

where σ_z^2 is the additive white Gaussian noise (AWGN) power at the receiver, $\gamma_{ij}[n] = \frac{P_i\rho_0\bar{\xi}_{ij}^2\alpha^n\beta_j}{\beta_j+1}$ and $\eta_{ij}[n] = P_i\rho_0(\frac{\alpha^n}{\beta_j+1} + \sigma_h^2(1-\alpha^n)) + \sigma_z^2H_j^2$.

Proof: Please refer to Appendix A. ■

It is noted that in the worst case, the estimation error is regarded as noise, which is increasing with respect to time. Therefore, given the locations $\mathbf{q}_j[n]$, the lower bound of SNR decreases with time.

D. Short-Packet Communication Model

To support the latency-sensitive tasks, short-packet communication is adopted. However, Shannon's capacity is applied under the assumption that the packet length is infinity and the decoding error probability equals zero. Therefore, it can not accurately capture the achievable data rate in short-packet communication. Moreover, it is assumed that the IoT devices transmit data at non-overlapping frequency channels with identical bandwidth B through frequency division multiple access (FDMA). Therefore, the achievable rate, in bits/second (bps), at the vehicle ($j=0$) and the UAV ($j=1$) from the i-th IoT device during the n-th time slot is given by [26] [30]

$$\begin{aligned} R_{ij}[n] =& B[\log_2(1+\Gamma_{ij}[n]) - \sqrt{\frac{V_{ij}[n]}{\delta B}}\frac{Q^{-1}(\epsilon)}{\ln 2}] \\ =& B\log_2(1+\Gamma_{ij}[n]) - \varsigma\sqrt{V_{ij}[n]}, \end{aligned} \tag{12}$$

where $V_{ij}[n]$ is the channel dispersion given by $V_{ij}[n] = 1-(1+\Gamma_{ij}[n])^{-2}$, $Q^{-1}(\cdot)$ is the inverse of the Gaussian Q-function, ϵ is the decoding error probability, and $\varsigma = \frac{Q^{-1}(\epsilon)}{\ln 2}\sqrt{\frac{B}{\delta}}$.

We assume that the computational data offloaded from a single IoT device can be partitioned into multiple smaller-size data which can be separately offloaded to the vehicle and the UAV, and executed in parallel [31]. It is also assumed that the IoT devices upload data only when being waken up by the vehicle or the UAV and scheduled for transmission, otherwise they remain in the silent mode for energy saving. The communication scheduling variable for the i-th IoT device in the n-th time slot is denoted as $a_{ij}[n]$. The i-th IoT device transmits data to the vehicle ($j=0$) or the UAV ($j=1$) in the n-th time slot if $a_{ij}[n]=1$ and keeps silent otherwise.

Since each data bit can be executed independently, the received data at the vehicle and the UAV in each time slot are immediately executable in the next slot. Therefore, the vehicle and the UAV only receive but do not process the computational data in the first time slot. In order to successfully execute all the offloaded data before the vehicle reaches the final location, the IoT devices do not offload in the last time slot. Furthermore, we also assume that each IoT device can communicate with at most one of the vehicle and the UAV in each time slot. Thus, we have the following constraints,

$$a_{ij}[n] \in \{0,1\}, \forall i \in \mathcal{K}, j \in \{0,1\}, n \in \mathcal{N}/N, \tag{13}$$

$$\sum_{j\in\{0,1\}} a_{ij}[n] \le 1, \forall i \in \mathcal{K}, n \in \mathcal{N}/N. \tag{14}$$

E. Computation Model

For each IoT device, denote the number of required CPU cycles for computing 1 bit data as C_i in cycles/bits, and the CPU frequency allocated by the vehicle ($j=0$) and the UAV ($j=1$) in the n-th time slot as $f_{ij}[n]$ in Hz. Then, the CPU frequency constraint can be expressed as

$$\sum_{i\in\mathcal{K}} f_{ij}[n] \le f_j^{max}, j \in \{0,1\}, n \in \mathcal{N}/1. \tag{15}$$

Due to the limited computation capacity of the vehicle and the UAV, the accumulative data from the n-th to the $(N-1)$-th time slots should not be larger than the accumulative CPU frequency from the $(n+1)$-th to the N-th time slots. Hence, the computation constraint is expressed as

$$\sum_{l=n}^{N-1} C_i a_{ij}[l]R_{ij}[l] \le \sum_{l=n+1}^{N} f_{ij}[l], \quad \forall i \in \mathcal{K}, j \in \{0,1\}, n \in \mathcal{N}/N. \tag{16}$$

This article has been accepted for publication in a future issue of this journal, but has not been fully edited. Content may change prior to final publication. Citation information: DOI10.1109/TVT.2022.3232841, IEEE Transactions on Vehicular Technology

More intuitively, the constraint can be interpreted as that the data received in the current time slot should be executed before the vehicle reaches the final location.

F. Problem Formulation

We aim to maximize the total amount of computation by jointly optimizing the communication scheduling $\mathbf{A} = \{a_{ij}[n], \forall i \in \mathcal{K}, j \in \{0,1\}, n \in \mathcal{N}/N\}$, the trajectories of the vehicle and the UAV $\mathbf{Q} = \{\mathbf{q}_j[n], j \in \{0,1\}, n = 1, ..., N+1\}$, and the computing resource $\mathbf{F} = \{f_{ij}[n], \forall i \in \mathcal{K}, j \in \{0,1\}, n \in \mathcal{N}/1\}$, subject to the mobility, connection and computation constraints. Therefore, the optimization problem is formulated as

$$\max_{\mathbf{A},\mathbf{Q},\mathbf{F}} \sum_{i=1}^{K} \sum_{j\in\{0,1\}} \sum_{n=1}^{N-1} a_{ij}[n] R_{ij}[n] \tag{17}$$
$$\text{s.t. } (1), (2), (3), (13), (14), (15), (16).$$

Note that problem (17) is a mix-integer non-convex optimization problem, which is difficult to obtain the optimal solution efficiently due to the following two reasons. First, the variables $a_{ij}[n]$ are binary. Second, even without $a_{ij}[n]$, $R_{ij}[n]$ in the objective function and constraint (16) are non-convex with respect to $q_j[n]$. To tackle these difficulties, in the following, we propose an alternative algorithm to obtain a high-quality solution.

IV. Proposed Solution to Problem (17)

In this section, we decompose problem (17) into two subproblems: communication scheduling as well as trajectory and computing resource optimization problems. With any given trajectory $\mathbf{Q}$ and computing resource $\mathbf{F}$, the communication scheduling $\mathbf{A}$ is optimized in the first subproblem through Lagrangian dual decomposition method. For any given communication scheduling $\mathbf{A}$, the trajectory $\mathbf{Q}$ and computing resource $\mathbf{F}$ are jointly optimized in the second subproblem by the SCA technique. Then, an alternative algorithm is proposed to solve the original problem (17).

A. Communication Scheduling Optimization

Given any trajectory $\mathbf{Q}$ and computing resource $\mathbf{F}$, problem (17) is transformed into the following problem,

$$\max_{\mathbf{A}} \sum_{i=1}^{K} \sum_{j\in\{0,1\}} \sum_{n=1}^{N-1} a_{ij}[n] R_{ij}[n] \tag{18}$$
$$\text{s.t. } (13), (14), (16).$$

It is noted that problem (18) is an integer programming, which can be solved by Branch and Bound algorithm. Although this method can obtain the optimal solution, it has high complexity. In order to solve this problem by a low-complex algorithm, we apply the Lagrangian dual decomposition method [32].

First, we relax the binary variables $a_{ij}[n]$ to continuous variables, i.e., $0 \le a_{ij}[n] \le 1$. Therefore, problem (18) is simplified to a linear programming problem as follows,

$$\max_{\mathbf{A}} \sum_{i=1}^{K} \sum_{j\in\{0,1\}} \sum_{n=1}^{N-1} a_{ij}[n] R_{ij}[n] \tag{19}$$
$$\text{s.t. } (14), (16),$$
$$0 \le a_{ij}[n] \le 1, \forall i \in \mathcal{K}, j \in \{0,1\}, n \in \mathcal{N}/N. \tag{19a}$$

Then, the Lagrangian function is given by

$$L(\mathbf{A}, \mathbf{\Lambda}) = \sum_{i=1}^{K} \sum_{j\in\{0,1\}} \sum_{n=1}^{N-1} \{a_{ij}[n] R_{ij}[n] - \lambda_{ij}[n] (\sum_{l=n}^{N-1} C_i a_{ij}[l] R_{ij}[l] - \sum_{l=n+1}^{N} f_{ij}[l])\}, \tag{20}$$

where $\mathbf{\Lambda} = \{\lambda_{ij}[l] \ge 0, \forall i \in \mathcal{K}, j \in \{0,1\}, l \in \mathcal{N}/N\}$ are the nonnegative dual variables. Since problem (19) is convex and satisfies the Slater's condition, strong duality holds between problem (19) and its dual problem, which is given by

$$\min_{\mathbf{\Lambda}} \max_{\mathbf{A}} L(\mathbf{A}, \mathbf{\Lambda}) \tag{21}$$
$$\text{s.t. } (14), (19a).$$

Therefore, solving problem (19) is equivalent to solving problem (21).

Note that the inner maximization problem in (21) can be reformulated as

$$\max_{\mathbf{A}} \sum_{i=1}^{K} \sum_{j\in\{0,1\}} \sum_{n=1}^{N-1} a_{ij}[n] \Omega_{ij}[n] \tag{22}$$
$$\text{s.t. } (14), (19a),$$

where $\Omega_{ij}[n] = R_{ij}[n](1 - C_i \sum_{m=1}^{n} \lambda_{ij}[m])$ is constant. To maximize the objective function in problem (22) while satisfying the constraints (14) and (19a), the $a_{ij}[n]$, $\forall i \in \mathcal{K}, n \in \mathcal{N}/N$, with the largest coefficient $\Omega_{ij}[n]$ should be 1 and the others be 0. For any given $i \in \mathcal{K}$ and $m \in \mathcal{N}/N$, we can obtain the optimal $j_i^*[n]$ by solving the following problem,

$$j_i^*[n] = \arg \max_{j\in\{0,1\}} \Omega_{ij}[n]. \tag{23}$$

Then, the optimal $a_{ij}^*[n]$ is given by

$$a_{ij}^*[n] = \begin{cases} 1, & \text{if } j = j_i^*[n], \\ 0, & \text{otherwise.} \end{cases} \tag{24}$$

It can be seen that the solution to problem (22) also satisfies the integer constraint (13) in problem (18). Therefore, the solution to problem (18) is obtained by (24).

Next, for the outer minimization problem in (21), we adopt the subgradient-based method to update the dual variable as

$$\lambda_{ij}^{(r+1)}[l] = [\lambda_{ij}^{(r)}[l] - \mu^{(r)}(-\sum_{n=l}^{N-1} C_i a_{ij}[n] R_{ij}[n] + \sum_{n=l+1}^{N} f_{ij}[n]))]^+, \tag{25}$$

where $\mu^{(r)}$ is the step size in the r-th iteration and $[\cdot]^+$ denotes the projection on positive orthant. The dual variable $\mathbf{\Lambda}$ and the

This article has been accepted for publication in a future issue of this journal, but has not been fully edited. Content may change prior to final publication. Citation information: DOI10.1109/TVT.2022.3232841, IEEE Transactions on Vehicular Technology

communication scheduling variable $\mathbf{A}$ are updated iteratively until the objective function in problem (21) converges. The details of the algorithm are summarized in Algorithm 1.

Algorithm 1 Iterative algorithm for problem (21)

1: $r \leftarrow 0$
2: Initialize the dual variables $\lambda_{ij}^{(r)}[x]$.
3: **repeat**
4: Update the dual variables $\lambda_{ij}^{(r+1)}[x]$ by performing the gradient update in formula (25).
5: Obtain the solution of communication scheduling $a_{ij}^{*}[n]$ by formulas (23) and (24).
6: Update the local points $a_{ij}^{(r+1)}[n] \leftarrow a_{ij}^{*}[n]$.
7: $r \leftarrow r+1$.
8: **until** The objective value converges.

B. Trajectory and Computation Resource Optimization

With any given communication scheduling $\mathbf{A}$, problem (17) is transformed into

$$\max_{\mathbf{Q},\mathbf{F}} \sum_{i=1}^{K} \sum_{j\in\{0,1\}} \sum_{n=1}^{N-1} a_{ij}[n] R_{ij}[n] \tag{26}$$
$$\text{s.t. } (1),(2),(3),(15),(16).$$

Note that in the objective function and constraint (16), $R_{ij}[n]$ is neither convex nor concave with respective to $\mathbf{q}_j[n]$. Therefore, problem (26) is still non-convex, which is difficult to be directly solved in general. To tackle such challenge, we first introduce the slack variables $\mathbf{\Theta} = \{\theta_{ij}[n], \forall i \in \mathcal{K}, j \in \{0,1\}, n \in \mathcal{N}/N\}$, and thus problem (26) is transformed into

$$\max_{\mathbf{Q},\mathbf{F},\mathbf{\Theta}} \sum_{i=1}^{K} \sum_{j\in\{0,1\}} \sum_{n=1}^{N-1} a_{ij}[n] R_{ij}^{\theta}[n] \tag{27}$$
$$\text{s.t. } (1),(2),(3),(15),$$
$$\sum_{n=l}^{N-1} C_i a_{ij}[n] R_{ij}^{\theta}[n] \le \sum_{n=l+1}^{N} f_{ij}[n],$$
$$\forall i \in \mathcal{K}, j \in \{0,1\}, l \in \mathcal{N}/N, \tag{27a}$$
$$\theta_{ij}[n] \le \Gamma_{ij}[n],$$
$$\forall i \in \mathcal{K}, j \in \{0,1\}, n \in \mathcal{N}/N, \tag{27b}$$

where $R_{ij}^{\theta}[n] = B\log_2(1+\theta_{ij}[n]) - \varsigma\sqrt{1-(1+\theta_{ij}[n])^{-2}}$.

Then, we prove that solving problem (27) is equivalent to solving problem (26). Define $f(x) = b[x^3(1-x)^{-\frac{3}{2}} + 3x^2(1-x)^{-\frac{1}{2}}] - cx$, where b and c are positive constants.

Lemma 2: For $0 < x < 1$, $f(x) < 0$.

Proof: Please refer to Appendix B. ■

Based on Lemma 2, we have the following Proposition.

Proposition 1: $R_{ij}^{\theta}[n]$ is a monotonically increasing concave function with respect to $\theta_{ij}[n]$.

Proof: Please refer to Appendix C. ■

Based on Proposition 1, it can be verified that at the optimal solution to problem (27), the constraint (27b) can be satisfied with equality, otherwise the objective value of problem (27) can always be increased by increasing $\theta_{ij}[n]$. Therefore, problem (26) is equivalent to problem (27).

As can be seen, constraints (27a) and (27b) are still non-convex. To tackle such issue, the SCA technique is adopted, where the original function is approximated by a more tractable function at a given local point in each iteration. Denote $\mathbf{\Theta}^r = \{\theta_{ij}^r[n], \forall i \in \mathcal{K}, j \in \{0,1\}, n \in \mathcal{N}/N\}$ and $\mathbf{Q}^r = \{\mathbf{q}_j^r[n], j \in \{0,1\}, n = 1, ..., N+1\}$ as the given slack variables and trajectories of the vehicle and the UAV, respectively, in the r-th iteration. According to Proposition 1, $R_{ij}^{\theta}[n]$ is concave with respect to $\theta_{ij}[n]$. Since any concave function is globally upper-bounded by its first-order Taylor expansion at any given local point. Therefore, the upper bound of $R_{ij}^{\theta}[n]$ at the given local point $\mathbf{\Theta}^r$ in the r-th iteration can be expressed as

$$\begin{aligned} R_{ij}^{\theta}[n] &\le A_{ij}^r[n] + I_{ij}^r[n](\theta_{ij}[n] - \theta_{ij}^r[n]) \\ &\triangleq R_{ij}^{\theta,ub}[n], \forall i \in \mathcal{K}, j \in \{0,1\}, n \in \mathcal{N}/N, \end{aligned} \tag{28}$$

where $A_{ij}^r[n] = B\log_2(1+\theta_{ij}^r[n]) - \varsigma\sqrt{1-(1+\theta_{ij}^r[n])^{-2}}$ and $I_{ij}^r[n] = \frac{B}{\ln 2}(1+\theta_{ij}^r[n])^{-1} - \varsigma[1-(1+\theta_{ij}^r[n])^{-2}]^{-\frac{1}{2}}(1+\theta_{ij}^r[n])^{-3}$ are positive constants. Therefore, $R_{ij}^{\theta,ub}[n]$ is affine with respect to $\theta_{ij}[n]$.

Although $\Gamma_{ij}[n]$ is neither concave nor convex with respect to $\mathbf{q}_j[n]$, it is convex with respect to $\|\mathbf{q}_j[n] - \mathbf{w}_i\|^2$. Since any convex function is globally lower-bounded by its first-order Taylor expansion at any given local point. Therefore, the lower bound of $\Gamma_{ij}[n]$ at the given local point $\mathbf{Q}^r$ in the r-th iteration can be expressed as

$$\begin{aligned} \Gamma_{ij}[n] &\ge Q_{ij}^r[n] \\ &\quad - W_{ij}^r[n](\|\mathbf{q}_j[n] - \mathbf{w}_i\|^2 - \|\mathbf{q}_j^r[n] - \mathbf{w}_i\|^2) \\ &\triangleq \Gamma_{ij}^{lb}[n], \forall i \in \mathcal{K}, j \in \{0,1\}, n \in \mathcal{N}/N, \end{aligned} \tag{29}$$

where $Q_{ij}^r[n] = \frac{\gamma_{ij}[n]}{\sigma_z^2\|\mathbf{q}_j^r[n]-\mathbf{w}_i\|^2+\eta_{ij}[n]}$ and $W_{ij}^r[n] = \frac{\gamma_{ij}[n]\sigma_z^2}{(\sigma_z^2\|\mathbf{q}_j^r[n]-\mathbf{w}_i\|^2+\eta_{ij}[n])^2}$ are positive constants. Therefore, $\Gamma_{ij}^{lb}[n]$ is concave function with respect to $\mathbf{q}_j[n]$.

With any given local points $\mathbf{\Theta}^r = \{\theta_{ij}^r[n], \forall i \in \mathcal{K}, j \in \{0,1\}, n \in \mathcal{N}/N\}$ and $\mathbf{Q}^r = \{\mathbf{q}_j^r[n], j \in \{0,1\}, n = 1, ..., N+1\}$, according to the upper- and lower-bound expressions in formulas (28) and (29), problem (27) is approximated as

$$\max_{\mathbf{Q},\mathbf{F},\mathbf{\Theta}} \sum_{i=1}^{K} \sum_{j\in\{0,1\}} \sum_{n=1}^{N-1} a_{ij}[n] R_{ij}^{\theta}[n] \tag{30}$$
$$\text{s.t. } (1),(2),(3),(15),$$
$$\sum_{n=l}^{N-1} C_i a_{ij}[n] R_{ij}^{\theta,ub}[n] \le \sum_{n=l+1}^{N} f_{ij}[n],$$
$$\forall i \in \mathcal{K}, j \in \{0,1\}, l \in \mathcal{N}/N, \tag{30a}$$
$$\theta_{ij}[n] \le \Gamma_{ij}^{lb}[n],$$
$$\forall i \in \mathcal{K}, j \in \{0,1\}, n \in \mathcal{N}/N. \tag{30b}$$

In this problem, the objective function is concave, constraints (1), (15) and (30a) are linear, and the other constraints are all convex. Therefore, problem (30) is a convex optimization problem, which can be solved by standard optimization

This article has been accepted for publication in a future issue of this journal, but has not been fully edited. Content may change prior to final publication. Citation information: DOI10.1109/TVT.2022.3232841, IEEE Transactions on Vehicular Technology

method, such as interior-point method. Hence, problem (26) can be solved by alternatively optimizing problem (30) with local points $\mathbf{\Theta}^r$ and $\mathbf{Q}^r$ in each iteration. The details are summarized in Algorithm 2.

Algorithm 2 SCA-based algorithm for problem (30)

1: $r \leftarrow 0$
2: Initialize the slack variables $\theta_{ij}^r[n]$ and the trajectories of the vehicle and the UAV $\mathbf{q}_j^r[n]$.
3: **repeat**
4: Solve problem (30) with local points $\theta_{ij}^r[n]$ and $\mathbf{q}_j^r[n]$, and obtain the solution $\mathbf{q}_j^*[n]$, $\theta_{ij}^*[n]$ and $f_{ij}^*[n]$.
5: Update the local points $\mathbf{q}_j^{r+1}[n] \leftarrow \mathbf{q}_j^*[n]$ and $\theta_{ij}^{r+1}[n] \leftarrow \theta_{ij}^*[n]$.
6: $r \leftarrow r+1$.
7: **until** The objective value converges.

C. Overall algorithm

Based on Algorithm 1 and Algorithm 2, which solve the communication scheduling optimization as well as trajectory and computing resource optimization problems, respectively, an alternative algorithm is proposed to solve the original problem (17). First, in the $(r+1)$-th iteration, given the trajectory $\mathbf{Q}^r$ and the computing resource $\mathbf{F}^r$, problem (21) is solved to obtain the communication scheduling $\mathbf{A}^{r+1}$ by Algorithm 1. Then, with $\mathbf{A}^{r+1}$, problem (30) is solved to obtain $\mathbf{Q}^{r+1}$ and $\mathbf{F}^{r+1}$ by Algorithm 2. The iteration continues until the objective value of problem (17) converges. The details of the overall algorithm are summarized in Algorithm 3.

Algorithm 3 Overall algorithm for problem (17)

1: $r \leftarrow 0$
2: Initialize the trajectories of the vehicle and the UAV $\mathbf{q}_j^r[n]$ and the computing resource $f_{ij}^r[n]$.
3: **repeat**
4: Solve problem (21) with the local points $\mathbf{q}^r[n]$ and $f_{ij}^r[n]$ by Algorithm 1, and obtain the solution $a_{ij}^*[n]$.
5: Update the local point $a_{ij}^{r+1}[n] \leftarrow a_{ij}^*[n]$.
6: Solve problem (30) with the local point $a_{ij}^{r+1}[n]$ by Algorithm 2, and obtain the solution $\mathbf{q}_j^*[n]$ and $f_{ij}^*[n]$.
7: Update the local points $\mathbf{q}^{r+1}[n] \leftarrow \mathbf{q}_j^*[n]$ and $f_{ij}^{r+1}[n] \leftarrow f_{ij}^*[n]$.
8: $r \leftarrow r+1$.
9: **until** The objective value converges.

D. Convergence and Complexity Analysis

It can be verified that the objective value of problem (17) is non-decreasing after each iteration of Algorithm 3. Moreover, the objective function of problem (17) is upper-bounded by a finite value. Thus, the convergence of Algorithm 3 is guaranteed.

Note that the complexity of Algorithm 3 lies in solving problems (21) and (30). The former one is solved by dual decomposition method in Algorithm 1. Its complexity is $O(2I_dK(N-1))$, where I_d denotes the number of iterations required by the dual method. The later one is solved by interior-point method in Algorithm 2. Therefore, the complexity is roughly given by $O(I_i(2(N+1)+4K(N-1))^{3.5})$, where I_i represents the number of iterations required by Algorithm 2. Hence, the complexity of the overall algorithm is $O(2I_dK(N-1)+I_i(2(N+1)+4K(N-1))^{3.5})$.

V. Simulation Results

In this section, numerical results are provided to verify the effectiveness of the proposed algorithm. According to the practical vehicle, the height of the vehicle is set as $H_0 = 1.5$ m. Considering the channel quality and energy consumption of the UAV, the altitude of the vehicle-mounted UAV is set as $H_1 = 40$ m [21]. The vehicle is assumed to travel along the straight line between the initial location $\mathbf{q}_I = [0,0]^T$ m and the final location $\mathbf{q}_F = [0,1000]^T$ m. In order to guarantee that the UAV can fly back to the vehicle at the final location, the maximum speeds of the vehicle and the UAV are set as $V_0^{max} = 20$ m/s [33] and $V_1^{max} = 30$ m/s [34], respectively. We consider the UAV-aided vehicular short-packet communication and edge computing system with $K = 20$ IoT devices that are randomly and uniformly distributed within a square area of 1×1 km^2. For ease of analysis, it is assumed that all the IoT devices have identical property, i.e., they transmit data at the same power $P_i = 0.01$ W and have the same computation requirement for 1 bit data $C_i = 1000$ cycles/bit [13]. The other parameters are set as follows: the channel power gain $\rho_0 = -60$ dB at the reference distance of $d_0 = 1$ m, the temporal fading coefficient $\alpha = 0.98$ [29], the Rician factors $\beta_0 = 1$ and $\beta_1 = 2$ [35], the variance of channel estimation error $\sigma_h^2 = 1$, the received noise power $\sigma_z^2 = -80$ dBm, the decoding error probability $\epsilon = 10^{-9}$, and the channel bandwidth $B = 5$ MHz. Unless otherwise stated, the simulation parameters are summarized in Table II.

For comparison, we consider two benchmark algorithms, namely, 1) particle swarm optimization (PSO) based algorithm, in which each particle represents the communication scheduling of all the IoT devices in every time slot; 2) greedy-based algorithm, in which the IoT devices are assigned to the one with the highest throughput among the vehicle and the UAV in current time slot, if both the vehicle and the UAV satisfy the constraints.

First, we study the convergence of the proposed algorithm in Fig. 2. It shows that the objective value increases quickly and the proposed algorithm converges in a few iterations. This demonstrates the convergence analysis in Section IV-D. As a comparison, the convergence of the greedy-based algorithm can not be guaranteed. That is because it only makes the best offloading decision for the devices in current time slot, but not the whole procedure, which results in a local optimal communication scheduling. Therefore, the convergence of the proposed algorithm is better than that of the greedy-based algorithm.

To validate the proposed algorithm, Fig. 3 shows the optimized trajectories under different computing resource of UAV f_1^{max}. It can be seen that the UAV first serves the IoT devices above the road, and then serves those below the road. The

This article has been accepted for publication in a future issue of this journal, but has not been fully edited. Content may change prior to final publication. Citation information: DOI10.1109/TVT.2022.3232841, IEEE Transactions on Vehicular Technology

TABLE II
SIMULATION PARAMETERS

Parameter	Description	Value
K	Number of IoT devices	4
δ	Time slot length	1s
ρ_0	Channel power gain at the reference distance of 1m	-60 dB
B	Channel bandwidth	5 MHz
α	Temporal fading coefficient	0.98
β_0	Rician factor of the vehicle's channel	1
β_1	Rician factor of the UAV's channel	2
ϵ	Decoding error probability	10^{-9}
σ_h^2	Variance of channel estimation error	1
σ_z^2	Noise power at the receiver	-80 dBm
P_i	Transmit power of the i-th IoT device	0.01 W
C_i	Required CPU cycles for computing 1 bit data	1000 cycle/bit
$\mathbf{q}_I$	Initial location of the vehicle	$[0,0]^T$ m
$\mathbf{q}_F$	Final location of the vehicle	$[0,1000]^T$ m
H_0	Height of the vehicle	1.5 m
H_1	Altitude of the UAV	40 m
V_0^{max}	Maximum speed of the vehicle	20 m/s
V_1^{max}	Maximum speed of the UAV	30 m/s

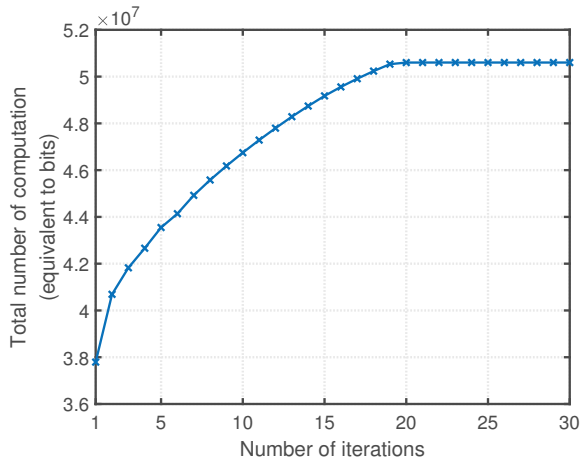

Fig. 2. Convergence of Algorithm 3.

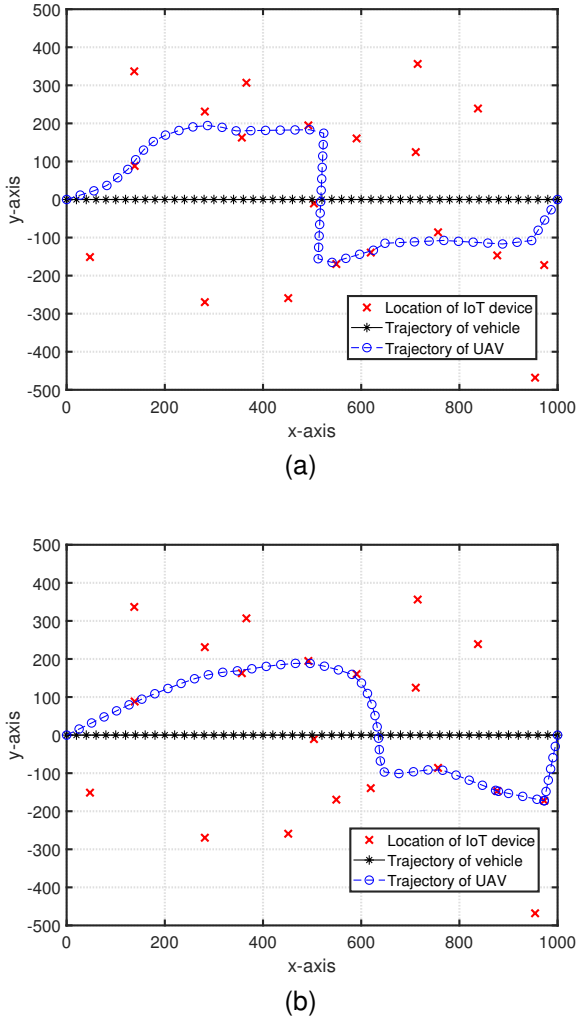

Fig. 3. Trajectories of the vehicle and the UAV in the network with 20 IoT devices. (a) $T = 50$ s, $f_0^{max} = 2$ GHz, $f_1^{max} = 10$ MHz. (b) $T = 50$ s, $f_0^{max} = 2$ GHz, $f_1^{max} = 1$ GHz.

reason is that there are more near devices below the road when $x > 500$ m, which can offload more computational data. Furthermore, by comparing Fig. 3(a) and Fig. 3(b), we can see that the UAV prefers to fly close to the near devices when its computing resource is sufficient, otherwise it trends to be close to the far ones. That is because when the computing resource of the UAV is inadequate, the vehicle can execute more data offloaded from the near IoT devices than the UAV, and the UAV can increase the total amount of computation by processing the data offloaded from the far devices. On the contrary, when the computing resource of UAV is sufficient, it can fly close to the devices to achieve more data than the vehicle. Therefore, the UAV would like to execute the data offloaded from the near devices to save the flight time for the computation. In addition, as observed from Fig. 3(b), the UAV with sufficient computing resource would like to serve more devices above the road even though the devices below the road are closer. That is because the optimization problem is formulated based on the lower bound of SNR under the time-varying channel. The channel estimation becomes less accurate over time, and thus the lower bound of SNR decreases with respect to time. Therefore, the IoT devices that the UAV encounters first (the devices above the road) can transmit more computational data.

In order to further investigate the impact of the vehicle travel time and the computing resource on the total amount of computation, we simulate the proposed algorithm under different vehicle travel time and computing resource of UAV, respectively, as shown in Fig. 4. Since the distances between the curves in bits are too close to observe, we plot the total amount of computation in dB on the following figures. As can be seen from Fig. 4(a), the total amount of computation increases with the vehicle travel time, since the vehicle and the UAV have more time to execute more data. However, the increase rate generally slows down over the vehicle travel time. It is because the UAV is able to fly close enough to

This article has been accepted for publication in a future issue of this journal, but has not been fully edited. Content may change prior to final publication. Citation information: DOI10.1109/TVT.2022.3232841, IEEE Transactions on Vehicular Technology

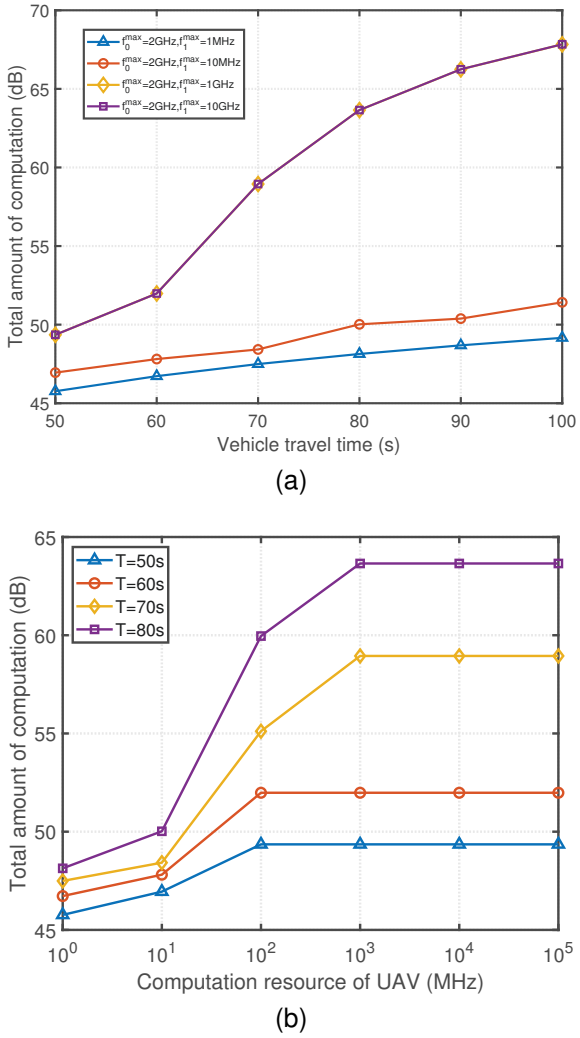

Fig. 4. Total amount of computation under different conditions. (a) vehicle travel time. (b) computing resource of UAV.

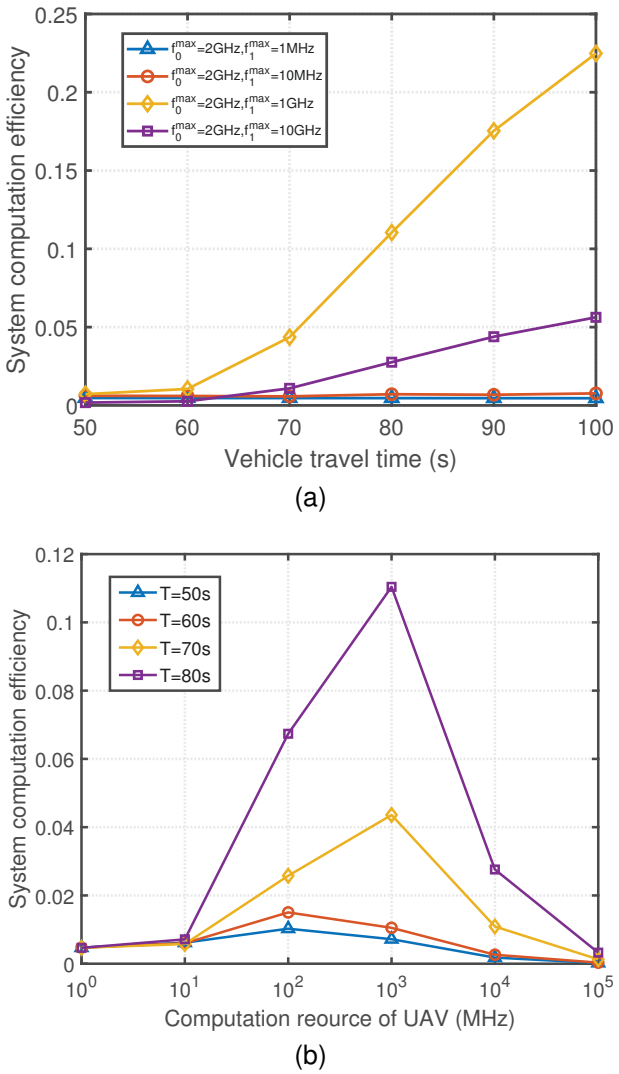

Fig. 5. System computation efficiency under different conditions. (a) vehicle travel time. (b) computing resource of UAV.

the served devices in less time. More time can only increase the hovering time, which yields a limited improvement in the amount of computation. From Fig. 4(b), one can observe that the total amount of computation first increases with the computing resource of UAV, and then stays unchanged when the computing resource of UAV reaches a certain level. That is because the UAV can execute more computational data with the increase of its computing resource. However, when it comes to a certain level, the computing resource of the vehicle and UAV exceeds the maximum computation requirement of the IoT devices.

Then, we plot the system computation efficiency under different vehicle travel time and computing resource of UAV, respectively, in Fig. 5, to further illustrate the analysis of Fig. 4. As observed from Fig. 5 (a), due to the increase of the total amount of computation, the system computation efficiency also increases with respect to the vehicle travel time. This is consistent with the above analysis of Fig. 4(a). Besides, one can also see that when the computing resource of UAV is 10GHz, the system computation efficiency is less than that when the computing resource of UAV is smaller. Moreover, from Fig. 5(b), it can be observed that the system computation efficiency first increases and then decreases with the computing resource of UAV. These verify the above analysis that as the computing resource of UAV increases, the system computing resource exceeds the maximum computation requirement of the IoT devices.

For showing the impact of the time-varying channel and the short-packet communication on the system, we compare three schemes in Fig. 6, namely, 1) Scheme I: both the time-varying channel and the short-packet communication are considered as in this paper; 2) Scheme II: the channel dispersion $V_{ij}[n]$ in the achievable rate of the short-packet communication is approximated as 1 [36]; 3) Scheme III: the time-varying channel is not considered [37]. It can be observed that Scheme III can achieve the most amount of computation, and Scheme II achieves the least. The reasons are as follows. First, the achievable rate of the approximation method in Scheme II is lower than that in the other two schemes. Therefore, when the computing resource is sufficient, the amount of computation in Scheme II is lower. Second, the Scheme III only considers

This article has been accepted for publication in a future issue of this journal, but has not been fully edited. Content may change prior to final publication. Citation information: DOI10.1109/TVT.2022.3232841, IEEE Transactions on Vehicular Technology

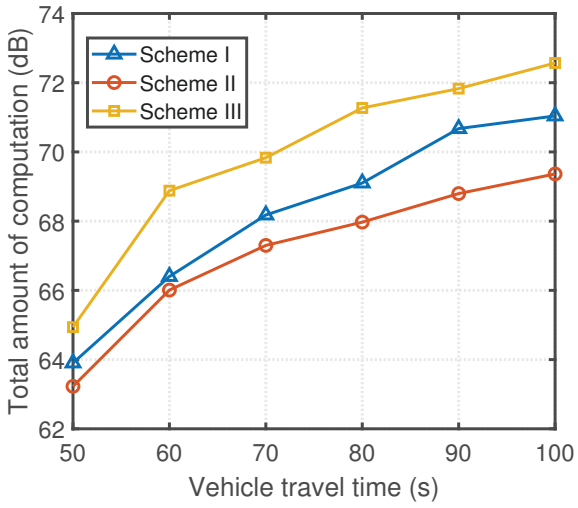

Fig. 6. Total amount of computation in different schemes.

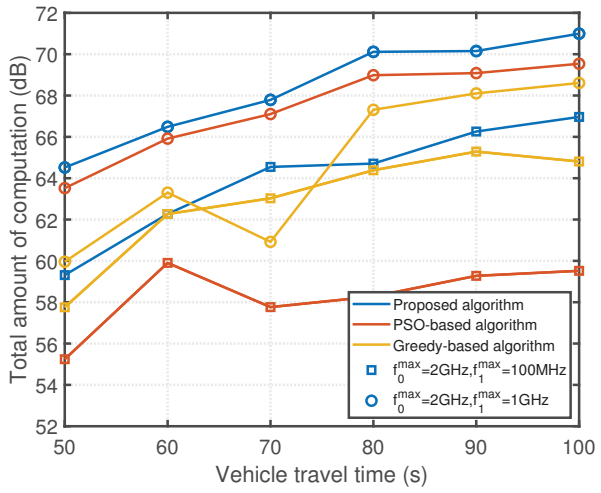

Fig. 7. Algorithm comparison under different conditions.

the large-scale fading, and thus the CSI is assumed to be accurate. Hence, compared with Scheme I and Scheme II, the IoT devices in Scheme III achieve the largest transmit rate. As a result, the system in Scheme III can process more computational data when the computing resource is sufficient. Although the system in Scheme I processes less data than that in Scheme III, Scheme I is more practical and can guarantee that the system at least completes this amount of computation. In addition, one can see that the performance gap between Scheme I and Scheme II increases with respect to the vehicle travel time. That is because the discrepancy between the achievable rates of Scheme I and Scheme II accumulates over the vehicle travel time. Moreover, since Scheme II adopts approximation method, the optimization results in Scheme I are more accurate than that in Scheme II.

To demonstrate the effectiveness of the proposed algorithm, we compare it with PSO-based algorithm and greedy-based algorithm in Fig. 7. It can be seen that the proposed algorithm performs better than its counterparts. It achieves more amount of computation under different vehicle travel time and computing resource of UAV. Moreover, since the PSO and the greedy algorithms are heuristic, the performances of the PSO-based and the greedy-based algorithms are not stable. Due to the heuristics, they fluctuate in Fig. 7, especially the greedy-based algorithm. Therefore, compared with the other two algorithms, the proposed algorithm is more stable.

VI. Conclusion

In this paper, we have proposed a novel UAV-aided VEC system architecture, where the on-board UAV assists the vehicle in executing the computational data offloaded from the roadside IoT devices. Through the first-order Gauss-Markov process, we have derived the lower bound of SNR under the time-varying Rician fading channel. Moreover, short packet communication has been applied to guarantee the low latency of the system. Based on these settings, we have formulated an optimization problem to maximize the total amount of computation by jointly optimizing the communication scheduling, the trajectories of the vehicle and on-board UAV, and the computing resource. This optimization problem is a mix-integer non-convex problem, which is challenging to solve. As such, we have decomposed the problem into two subproblems: communication scheduling, and trajectory and computing resource optimization problems. To solve these subproblems efficiently, we have proposed two algorithms by applying the Lagrangian dual decomposition method and SCA technique, respectively. Then an alternative algorithm has been proposed based on these two algorithms. Numerical results have shown that the on-board UAV prefers to fly close to the IoT devices it encounters first, since the lower bound of SNR decreases with respect to time in the time-varying fading channel. Furthermore, we have also illustrated that the proposed algorithm can improve the total amount of computation as compared to other benchmark algorithms.

Appendix A
Proof of the Lemma 1

For ease of exposition, we omit the indices of time slot, IoT device, vehicle and UAV in this proof. Denote S as the signal transmitted by the IoT device, and thus the received signal at the vehicle or UAV is given by

$$U = PHS + Z = P(\bar{H} + \widetilde{H})S + Z, \tag{31}$$

where $\mathbb{E}[S^2] = 1$, Z is the AWGN following the complex Gaussian distribution with zero mean and σ_z^2 variance.

The mutual information between U and S is given by

$$I(S;Y) = h(S) - h(S|U), \tag{32}$$

where $h(S) = \frac{1}{2}\log(2\pi eP)$ is a fixed value. Therefore, in order to obtain the lower bound of $I(S;Y)$, we need to find an upper bound of $h(S|U)$.

For any real number ω, the conditional entropy $h(S|U) = h(S-\omega U|U)$, and $h(S-\omega U|U) \leq h(S-\omega U)$ [38]. Therefore, we have

$$h(S|U) \leq h(S-\omega U) \leq \frac{1}{2}\log(2\pi eVar(S-\omega U)). \tag{33}$$

This article has been accepted for publication in a future issue of this journal, but has not been fully edited. Content may change prior to final publication. Citation information: DOI10.1109/TVT.2022.3232841, IEEE Transactions on Vehicular Technology

To minimize the RHS of the second inequality, ω is properly chosen such that ωU is the linear minimum mean-square error (LMMSE) estimate of S in terms of U, which is given by

$$\omega = \frac{\mathbb{E}[SU]}{\mathbb{E}[U^2]} = \frac{P\bar{H}}{P\bar{H}^2 + P\sigma_{\widetilde{H}}^2 + \sigma_z^2}. \tag{34}$$

By substituting (34) into (33), one can have

$$h(S|U) \leq \frac{1}{2}\log(2\pi e \frac{P_i\bar{H}}{P_i\bar{H}^2 + P\sigma_{\widetilde{H}}^2 + \sigma_z^2}). \tag{35}$$

Hence, the lower bound of the mutual information between S and U can be expressed as

$$\begin{aligned} I(S;Y) &= h(S) - h(S|U) \\ &\geq \frac{1}{2}\log(2\pi eP) - \frac{1}{2}\log(2\pi e \frac{P\bar{H}}{P\bar{H}^2 + P\sigma_{\widetilde{H}}^2 + \sigma_z^2}) \\ &= \frac{1}{2}\log(1 + \frac{P\bar{H}^2}{P\sigma_{\widetilde{H}}^2 + \sigma_z^2}). \end{aligned} \tag{36}$$

Therefore, the lower bound of SNR in time-varying Rician fading channel between the i-th IoT device and the vehicle as well as the UAV in the n-th time slot is given by

$$\Gamma_{ij}[n] = \frac{P_i\bar{h}_{ij}^2[n]}{P_i\sigma_{\widetilde{h}_{ij}[n]}^2 + \sigma_z^2}. \tag{37}$$

Thus, we complete the proof.

Appendix B
Proof of the Lemma 2

The first-order and second-order derivatives of $f(x)$ are given by

$$\begin{aligned} f' =& b[\frac{3}{2}x^3(1-x)^{-\frac{5}{2}} + \frac{9}{2}x^2(1-x)^{-\frac{3}{2}} \\ &+ 6x(1-x)^{-\frac{1}{2}}] - c, \end{aligned} \tag{38}$$

$$\begin{aligned} f'' =& b[\frac{15}{4}x^3(1-x)^{-\frac{7}{2}} + \frac{45}{4}x^2(1-x)^{-\frac{5}{2}} \\ &+ 12x(1-x)^{-\frac{3}{2}} + 6(1-x)^{-\frac{1}{2}}]. \end{aligned} \tag{39}$$

It is noted that $f'' > 0$ for $0 < x < 1$. Therefore, f' is a monotonically increasing function for $0 < x < 1$. Moreover, $\lim_{x\to 1} f' = -c < 0$. Hence, f is a monotonically decreasing function for $0 < x < 1$. Since $\lim_{x\to 0} f = 0$, one can have $f < 0$ for $0 < x < 1$. The proof is completed.

Appendix C
Proof of the Proposition 1

For ease of exposition, we simplify the notations $R_{ij}^{\theta}[n]$ and $\theta_{ij}[n]$ to R and θ, respectively, in this proof. The first-order and second-order derivatives of R are given by

$$R' = \frac{B}{\ln 2}(1+\theta)^{-1} - \varsigma[1-(1+\theta)^{-2}]^{-\frac{1}{2}}(1+\theta)^{-3}, \tag{40}$$

$$\begin{aligned} R'' =& \varsigma\{[1-(1+\theta)^{-2}]^{-\frac{3}{2}}(1+\theta)^{-6} \\ &+ 3[1-(1+\theta)^{-2}]^{-\frac{1}{2}}(1+\theta)^{-4}\} \\ &- \frac{B}{\ln 2}(1+\theta)^{-2}. \end{aligned} \tag{41}$$

Let $x = (1+\theta)^{-2}$, $b = \varsigma$, and $c = \frac{B}{\ln 2}$, then one can have $R'' = f$. Since $\theta > 0$, we have $0 < x < 1$. According to Lemma 2, owing to $R'' < 0$ for $0 < x < 1$, R is a concave function and R' is a monotonically decreasing function with respect to θ. Furthermore, we have $\lim_{\theta\to\infty} R' = 0$, and thus $R' > 0$. Therefore, R is a monotonically increasing concave function, which completes the proof.

References

[1] K. Wang, K. Yang, and C. S. Magurawalage, "Joint energy minimization and resource allocation in C-RAN with mobile cloud," *IEEE Transactions on Cloud Computing*, vol. 6, no. 3, pp. 760–770, 2018.

[2] T. Taleb, K. Samdanis, B. Mada, H. Flinck, S. Dutta, and D. Sabella, "On multi-access edge computing: A survey of the emerging 5G network edge cloud architecture and orchestration," *IEEE Communications Surveys & Tutorials*, vol. 19, no. 3, pp. 1657–1681, 2017.

[3] Y. Sun, S. Zhou, and Z. Niu, "Distributed task replication for vehicular edge computing: Performance analysis and learning-based algorithm," *IEEE Transactions on Wireless Communications*, vol. 20, no. 2, pp. 1138–1151, 2021.

[4] Y. Du, K. Yang, K. Wang, G. Zhang, Y. Zhao, and D. Chen, "Joint resources and workflow scheduling in UAV-enabled wirelessly-powered MEC for IoT systems," *IEEE Transactions on Vehicular Technology*, vol. 68, no. 10, pp. 10 187–10 200, 2019.

[5] T. Bai, J. Wang, Y. Ren, and L. Hanzo, "Energy-efficient computation offloading for secure UAV-edge-computing systems," *IEEE Transactions on Vehicular Technology*, vol. 68, no. 6, pp. 6074–6087, 2019.

[6] Y. Liu, S. Xie, and Y. Zhang, "Cooperative offloading and resource management for UAV-enabled mobile edge computing in power IoT system," *IEEE Transactions on Vehicular Technology*, vol. 69, no. 10, pp. 12 229–12 239, 2020.

[7] Q. Wu, J. Xu, Y. Zeng, D. W. K. Ng, N. Al-Dhahir, R. Schober, and A. L. Swindlehurst, "A comprehensive overview on 5G-and-beyond networks with UAVs: From communications to sensing and intelligence," *IEEE Journal on Selected Areas in Communications*, vol. 39, no. 10, pp. 2912–2945, 2021.

[8] W. R. Ghanem, V. Jamali, Y. Sun, and R. Schober, "Resource allocation for multi-user downlink MISO OFDMA-URLLC systems," *IEEE Transactions on Communications*, vol. 68, no. 11, pp. 7184–7200, 2020.

[9] S. He, W. Wang, H. Yang, Y. Cao, T. Jiang, and Q. Zhang, "State-aware rate adaptation for UAVs by incorporating on-board sensors," *IEEE Transactions on Vehicular Technology*, vol. 69, no. 1, pp. 488–496, 2020.

[10] S. Huang, M. Zhang, Y. Gao, and Z. Feng, "MIMO radar aided mmWave time-varying channel estimation in MU-MIMO V2X communications," *IEEE Transactions on Wireless Communications*, vol. 20, no. 11, pp. 7581–7594, 2021.

[11] N. Ishikawa, R. Rajashekar, C. Xu, M. El-Hajjar, S. Sugiura, L.-L. Yang, and L. Hanzo, "Differential-detection aided large-scale generalized spatial modulation is capable of operating in high-mobility millimeter-wave channels," *IEEE Journal of Selected Topics in Signal Processing*, vol. 13, no. 6, pp. 1360–1374, 2019.

[12] Y. Liu and O. Simeone, "Hyperrnn: Deep learning-aided downlink CSI acquisition via partial channel reciprocity for FDD massive MIMO," in *2021 IEEE 22nd International Workshop on Signal Processing Advances in Wireless Communications (SPAWC)*, 2021, pp. 31–35.

[13] Y. Sun, X. Guo, J. Song, S. Zhou, Z. Jiang, X. Liu, and Z. Niu, "Adaptive learning-based task offloading for vehicular edge computing systems," *IEEE Transactions on Vehicular Technology*, vol. 68, no. 4, pp. 3061–3074, 2019.

[14] X. Han, D. Tian, Z. Sheng, X. Duan, J. Zhou, W. Hao, K. Long, M. Chen, and V. C. M. Leung, "Reliability-aware joint optimization for cooperative vehicular communication and computing," *IEEE Transactions on Intelligent Transportation Systems*, vol. 22, no. 8, pp. 5437–5446, 2021.

[15] L. Xu, Z. Yang, H. Wu, Y. Zhang, Y. Wang, L. Wang, and Z. Han, "Socially driven joint optimization of communication, caching, and computing resources in vehicular networks," *IEEE Transactions on Wireless Communications*, vol. 21, no. 1, pp. 461–476, 2022.

[16] X. Huang, R. Yu, D. Ye, L. Shu, and S. Xie, "Efficient workload allocation and user-centric utility maximization for task scheduling in collaborative vehicular edge computing," *IEEE Transactions on Vehicular Technology*, vol. 70, no. 4, pp. 3773–3787, 2021.

[17] J. Cui, L. Wei, H. Zhong, J. Zhang, Y. Xu, and L. Liu, "Edge computing in VANETs-an efficient and privacy-preserving cooperative downloading scheme," *IEEE Journal on Selected Areas in Communications*, vol. 38, no. 6, pp. 1191–1204, 2020.

[18] N. Cheng, W. Xu, W. Shi, Y. Zhou, N. Lu, H. Zhou, and X. Shen, "Air-ground integrated mobile edge networks: Architecture, challenges, and opportunities," *IEEE Communications Magazine*, vol. 56, no. 8, pp. 26–32, 2018.

[19] L. Zhao, K. Yang, Z. Tan, X. Li, S. Sharma, and Z. Liu, "A novel cost optimization strategy for SDN-enabled UAV-assisted vehicular computation offloading," *IEEE Transactions on Intelligent Transportation Systems*, vol. 22, no. 6, pp. 3664–3674, 2021.

[20] L. Zhao, K. Yang, Z. Tan, H. Song, A. Al-Dubai, A. Y. Zomaya, and X. Li, "Vehicular computation offloading for industrial mobile edge computing," *IEEE Transactions on Industrial Informatics*, vol. 17, no. 11, pp. 7871–7881, 2021.

[21] H. Peng and X. Shen, "Multi-agent reinforcement learning based resource management in MEC- and UAV-assisted vehicular networks," *IEEE Journal on Selected Areas in Communications*, vol. 39, no. 1, pp. 131–141, 2021.

[22] C.-F. Liu, M. Bennis, M. Debbah, and H. V. Poor, "Dynamic task offloading and resource allocation for ultra-reliable low-latency edge computing," *IEEE Transactions on Communications*, vol. 67, no. 6, pp. 4132–4150, 2019.

[23] R. Dong, C. She, W. Hardjawana, Y. Li, and B. Vucetic, "Deep learning for hybrid 5G services in mobile edge computing systems: Learn from a digital twin," *IEEE Transactions on Wireless Communications*, vol. 18, no. 10, pp. 4692–4707, 2019.

[24] Z. Zhou, Z. Wang, H. Yu, H. Liao, S. Mumtaz, L. Oliveira, and V. Frascolla, "Learning-based URLLC-aware task offloading for Internet of health things," *IEEE Journal on Selected Areas in Communications*, vol. 39, no. 2, pp. 396–410, 2021.

[25] K. Wang, C. Pan, H. Ren, W. Xu, L. Zhang, and A. Nallanathan, "Packet error probability and effective throughput for ultra-reliable and low-latency UAV communications," *IEEE Transactions on Communications*, vol. 69, no. 1, pp. 73–84, 2021.

[26] C. She, C. Liu, T. Q. S. Quek, C. Yang, and Y. Li, "Ultra-reliable and low-latency communications in unmanned aerial vehicle communication systems," *IEEE Transactions on Communications*, vol. 67, no. 5, pp. 3768–3781, 2019.

[27] K. Chen, Y. Wang, J. Zhao, X. Wang, and Z. Fei, "URLLC-oriented joint power control and resource allocation in UAV-assisted networks," *IEEE Internet of Things Journal*, vol. 8, no. 12, pp. 10 103–10 116, 2021.

[28] Y. Cai, X. Jiang, M. Liu, N. Zhao, Y. Chen, and X. Wang, "Resource allocation for URLLC-oriented two-way UAV relaying," *IEEE Transactions on Vehicular Technology*, vol. 71, no. 3, pp. 3344–3349, 2022.

[29] C.-J. Chun, J.-M. Kang, and I.-M. Kim, "Adaptive rate and energy harvesting interval control based on reinforcement learning for SWIPT," *IEEE Communications Letters*, vol. 22, no. 12, pp. 2571–2574, 2018.

[30] Y. Polyanskiy, H. V. Poor, and S. Verdu, "Channel coding rate in the finite blocklength regime," *IEEE Transactions on Information Theory*, vol. 56, no. 5, pp. 2307–2359, 2010.

[31] Y. Mao, C. You, J. Zhang, K. Huang, and K. B. Letaief, "A survey on mobile edge computing: The communication perspective," *IEEE Communications Surveys Tutorials*, vol. 19, no. 4, pp. 2322–2358, 2017.

[32] Y. Ji, Z. Yang, H. Shen, W. Xu, K. Wang, and X. Dong, "Multicell edge coverage enhancement using mobile UAV-relay," *IEEE Internet of Things Journal*, vol. 7, no. 8, pp. 7482–7494, 2020.

[33] R. Zhang, R. Lu, X. Cheng, N. Wang, and L. Yang, "A UAV-enabled data dissemination protocol with proactive caching and file sharing in V2X networks," *IEEE Transactions on Communications*, vol. 69, no. 6, pp. 3930–3942, 2021.

[34] C. Zhan, H. Hu, X. Sui, Z. Liu, and D. Niyato, "Completion time and energy optimization in the UAV-enabled mobile-edge computing system," *IEEE Internet of Things Journal*, vol. 7, no. 8, pp. 7808–7822, 2020.

[35] J. Kang and W. Choi, "Novel codebook design for channel state information quantization in MIMO Rician fading channels with limited feedback," *IEEE Transactions on Signal Processing*, vol. 69, pp. 2858–2872, 2021.

[36] H. Ren, C. Pan, Y. Deng, M. Elkashlan, and A. Nallanathan, "Resource allocation for secure URLLC in mission-critical IoT scenarios," *IEEE Transactions on Communications*, vol. 68, no. 9, pp. 5793–5807, 2020.

[37] A. Ranjha and G. Kaddoum, "URLLC-enabled by laser powered UAV relay: A quasi-optimal design of resource allocation, trajectory planning and energy harvesting," *IEEE Transactions on Vehicular Technology*, vol. 71, no. 1, pp. 753–765, 2022.

[38] M. Medard, "The effect upon channel capacity in wireless communications of perfect and imperfect knowledge of the channel," *IEEE Transactions on Information Theory*, vol. 46, no. 3, pp. 933–946, 2000.

Shuai Shen received his M.S. degree from the School of Information and Control Engineering of China University of Mining and Technology, Xuzhou, China, in 2019. He is currently pursuing the Ph.D. degree in the School of Information and Communication Engineering, University of Electronic Science and Technology of China, Chengdu, China. His research interests include resource efficiency of wireless communications, unmanned aerial vehicle communications and multi-access edge computing.

Kun Yang received his PhD from the Department of Electronic & Electrical Engineering of University College London (UCL), UK. He is currently a Chair Professor in the School of Computer Science & Electronic Engineering, University of Essex, leading the Network Convergence Laboratory (NCL), UK. He is also an affiliated professor at UESTC, China. Before joining in the University of Essex at 2003, he worked at UCL on several European Union (EU) research projects for several years. His main research interests include wireless networks and communications, IoT networking, data and energy integrated networks and mobile computing. He manages research projects funded by various sources such as UK EPSRC, EU FP7/H2020 and industries. He has published 300+ papers and filed 20 patents. He serves on the editorial boards of both IEEE (e.g., IEEE TNSE, IEEE ComMag, IEEE WCL) and non-IEEE journals (e.g., Deputy EiC of IET Smart Cities). He is a Member of Academia Europaea (MAE). He is a Fellow of IEEE (2023), a Fellow of IET and a Fellow of BCS. He is an IEEE ComSoc Distinguished Lecturer (2020-2021).

Kezhi Wang received Ph.D. degree in Engineering from the University of Warwick, U.K. He was with University of Essex and Northumbria University, U.K. Currently he is a Senior Lecturer with Department of Computer Science, Brunel University London, U.K. His research interests include wireless communications, signal processing, mobile edge computing and machine learning. He was a co-recipient of the IEEE ComSoc Leonard G. Abraham Prize in 2022.

Guopeng Zhang received the bachelor's degree from the School of Computer Science, Jiangsu Normal University, Xuzhou, China, in 2001, the master's degree from the School of Computer Science, South China Normal University, Guangzhou, China, in 2005, and the Ph.D. degree from the School of Communication Engineering, Xidian University, Xi'an, China, in 2009. He was with ZTE Corporation Nanjing Branch for one year. In 2009, he joined the China University of Minin and Technology, Xuzhou, China, where he is currently a Professor with the School of Computer Science and Technology. He manages research projects funded by various sources, such as the National Natural Science Foundation of China. He has authored or coauthored more than 60 journal and conference papers. His main research interests include distributed computing and machine learning.